J Pharm Biopharm Res, 2023, 4(2): 326-339
DOI: 10.25082/JPBR.2022.02.004

RESEARCH ARTICLE

(*E*)-2-Benzylidenecyclanones: Part XVII [1]. An LC-MS study of microsomal transformation reactions of (*E*)-2-[(4'-methoxyphenyl)methylene]-benzosuberon -1-one: A cyclic chalcone analog

Fatemeh Kenari[1] **Szilárd Molnár**[2] **Zoltán Pintér**[1] **Sobhan Bitaraf**[1] **Pál Perjési**[1*]

[1] Institute of Pharmaceutical Chemistry, University of Pécs, H-7624, Pécs, Hungary
[2] Research Institute for Viticulture and Oenology, University of Pécs, H-7634, Hungary

Correspondence to: Pál Perjési, Institute of Pharmaceutical Chemistry, University of Pécs, H-7624, Pécs, Hungary; Email: pal.perjesi@gytk.pte.hu

Received: January 18, 2023;
Accepted: March 18, 2023;
Published: March 22, 2023.

Citation: Kenari F, Molnár S, Pintér Z, *et al*. (*E*)-2-Benzylidenecyclanones: Part XVII. An LC-MS study of microsomal transformation reactions of (*E*)-2-[(4'-methoxyphenyl)methylene]-benzosuberon-1-one: A cyclic chalcone analog. *J Pharm Biopharm Res*, 2023, **4**(2): 326-339.
https://doi.org/10.25082/JPBR.2022.02.004

Abstract: Biotransformation of the antiproliferative (*E*)-2-[(4'-methoxyphenyl)methylene]-benzosuberon-1-one (**2c**) was studied using rat liver microsomes. As a result of the CYP-catalyzed transformations, one monooxygenated (**2c+O**) and the demethylated (**2c-CH$_2$**) metabolites were identified by HPLC-MS. (*E*)-2-[(4'-methoxyphenyl)methylene]-benzosuberon-1-ol, the expected product of rat liver microsomal carbonyl reductase, was not found in the incubates. Microsomal GST-catalyzed reaction of the compound resulted in formation of diastereomeric GST-conjugates. Under the present HPLC conditions, the diastereomeric adducts were separated into two chromatographic peaks (**2c-GSH-1** and **2c-GSH-2**).

Keywords: chalcone, benzosuberone, microsome, CYP, chalcone reductase, glutathione, microsomal glutathione transferase

1 Introduction

Chalcones (Figure 1) are intermediary compounds of the biosynthetic pathway of a very large and widespread group of plant constituents known collectively as flavonoids [2]. Among the naturally occurring chalcones and their synthetic analogs, several compounds displayed cytotoxic (cell growth inhibitor) activity toward cultured tumor cells. Chalcones are also effective *in vivo* as cell proliferating inhibitors, antitumor promoting, anti-inflammatory and chemopreventive agents [3–5]. The chalcone structure can be divided into three structural units; the aromatic rings A and B and the propenone linker. Modifying any of them can tune the main feature of interactions of the synthetic chalcones towards the non-covalent or the covalent pathway.

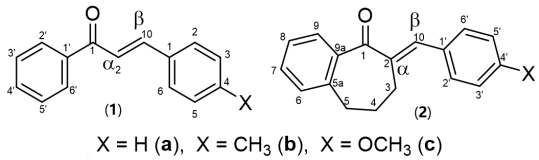

Figure 1 Structure and numbering of 4-X-chalcones (**1**) and (*E*)-2-[(4'methoxyphenyl) methylene]-1-benzosuberones (**2**)

In our previous studies, we have investigated how the substitution of the B-ring and the ring size (n = 0, 5, 6, 7) of some cyclic chalcone analogs affect their cancer cell cytotoxic effect [6–8]. Comparison of the average IC$_{50}$ values of the series, the benzosuberone (n = 7) (**2**) analogs (Figure 1) displayed the most prosperous data against the investigated murine and human tumor cell lines. In particular, the (*E*)-2-[(4-methoxyphenyl)methylene]-1-benzosuberone (**2c**) had the most remarkable cytotoxicity [6, 7].

In consecutive publications, we have performed cell cycle analysis of Jurkat cells exposed to equitoxic doses of **2c** and its methyl-substituted counterpart **2b**. Compound **2c** showed to cause an immediate G1 lift and G2/M arrest, followed by hypoploidity and aneuploidy. Such a remarkable effect of **2b** on the G1 and G2 checkpoints could not be observed [9, 10]. TLC and HPLC analysis showed the compounds to have intrinsic reactivity towards GSH [9, 11]. However, the two compounds had different effects on the thiol status of the cells. Compound **2c** significantly increased the oxidized glutathione (GSSG) level. On the contrary, **2b** increased the GSH level, indicating enhanced cellular antioxidant potency [12].

Although chalcones are a family of compounds with several beneficial biological activities, a limited number of metabolism studies of the compounds can be found in the literature.

Microsomal oxidation of chalcone and *(E)*-4-phenyl-3-buten-2-one, for example, resulted in the formation of aromatic hydroxylated metabolites [13]. In another publication of the research group, microsomal reduction of the carbonyl function of the compound was reported [14]. Incubation of the chemoprevention agent licochalcone A with human liver microsomes also resulted in oxygenated Phase I metabolites [15]. Similar results were obtained while investigating 8-prenylnaringenin [16].

In an earlier publication, we reported intestinal elimination and Phase 2 metabolism of 4'-hydroxy-4-methoxychalcone and its bis-Mannich analog in the rat. HPLC-MS analysis of the perfusates indicated the presence of glucuronide, sulfate, and glutathione conjugates of the parent molecules [17]. To compare GSH reactivity, two bis-Mannich bases of two 4'-hydroxychalcones were synthesized and reacted with GSH under non-cellular conditions. At pH values below 8.0, the two bis-Mannich bases showed higher GSH reactivity than two 4'-hydroxychalcones [18].

Previously demonstrated intrinsic reactivity of **2b** and **2c** towards GSH [9, 11] might play a role in their cancer cell cytotoxic effects. Oxidation of GSH to GSSG or chemical modification of the SH group of the tripeptide causes a change in the redox potential of the GSSG/2GSH system. Previously, a correlation has been found between the cell cycle, the condition of the cell (stressed, apoptotic, etc.), and the GSSG/2GSH ratio. For instance, in cell proliferation (E_{hc} = ˜-240 mV), in cell differentiation (E_{hc} = ˜-200 mV), and in apoptosis (E_{hc} = ˜-170 mV), which can be applicable for a better understanding of oxidative stress [19, 20]. Thus, changes in the GSSG/2GSH ratio are fundamental in controlling signal transduction that supports cell cycle regulation and other cellular processes [21, 22].

To investigate if **2b** and **2c** or their reactive metabolites react with thiols under cellular conditions, microsomal incubation of the compounds in the presence of reduced glutathione (GSH) was performed. The incubations were analyzed for the expected derivatives by HPLC-UV and HPLC-MS methods.

Microsomes are fragments of endoplasmic reticulum and attached ribosomes that are isolated together when homogenized cells are centrifuged. Microsomal enzymes are typically found in the smooth endoplasmic reticulum, primarily in the liver, but also in the kidney, intestinal mucosa, and lung. There are several microsomal enzymes, including flavin monooxygenases (FMO), cytochrome P450s (CYP), NADPH cytochrome c reductase, UDP glucuronyl transferases (UGT), glutathione-S-transferases (GST), epoxide hydrolases, among others. Hence, hepatic microsomes are commonly used to study the metabolic fate of drugs, as the liver is one of the major organs responsible for enzymatic drug elimination [23].

2 Materials and methods

2.1 Chemicals and reagents

(*E*)-2-[(4-methoxyphenyl)methylene]-1-benzosuberone (**2c**) was synthesized as previously published [6]. Its structure was characterized by IR and NMR spectroscopy [24]. The purity and structures of the investigated sample were verified by HPLC-MS (Figure 2 and 3). Male rat pooled liver microsome 10 mg, magnesium chloride, 25mm syringe filters nylon membrane, pore size 0.45 μm, and ß-nicotinamide adenine dinucleotide 2'-phosphate reduced tetrasodium salt hydrate (NADPH) were purchased from Sigma Aldrich (Budapest, Hungary). Alamethicin and reduced L-glutathione were obtained from Cayman Chemicals and ITW reagents. Methanol CHROMASOLV HPLC grade was obtained from Honeywell (Hungary). Trifluoroacetic acid was obtained from VWR (Budapest, Hungary), and formic acid from Fischer Chemicals (Budapest, Hungary). Deionized water for use in HPLC and HPLC-MS measurements was purified by Millipore Direct-QTM at the Institute of Pharmaceutical Chemistry (University of Pécs). Phosphate buffered Saline (PBS) pH 7.4 was prepared freshly on the day of incubation based on the 2014 Cold Spring Harbor Laboratory press method [25]. Mobile phases used for HPLC measurements were degassed by an ultrasonic water bath before use.

2.2 Light-initiated isomerization of 2c

Freshly prepared 6.5 $\times$ 10^{-3} M solution of **2c** in HPLC-grade methanol was subjected to scattered laboratory light for one week. The solution was analyzed by HPLC-UV and HPLC-MS.

2.3 Microsomal incubations

490μL PBS was mixed with 50μL of rat liver microsome (20 mg/mL protein) and 10 μL of alamethicin in methanol (50 μg/mg protein) and was left on ice for 15 minutes for microsomal activation. Then 100μL of NADPH solution (2.0 μmol/mL final concentration) was added, and the solution vortexed to mix well. 25μL of a freshly prepared acetonitrile solution of **2c**

(final concentration 0.25 μmol/mL) and 100μL of $MgCl_2$ solution (final concentration of 5.0 μmol/mL) were added. After each addition, the solution was vortexed. The incubation volume was set to a total of 980 μL by the addition of 205 μL of PBS and left in a 37°C water bath for 3 minutes. Then 20 μL of GSH solution in PBS (final concentration of 5.0 μmol/mL) was added to bring the final volume to 1.0 mL. The mixture was vortex mixed for 10 seconds, taken to a shaking water bath, and kept in it for the incubation period (120 minutes). 150 μL samples were taken at 0, 15, 30, 60, and 90-minute timepoints. (The 0-minute points were considered the time of placement of the incubates into the water bath.) 150 μL ice-cold methanol was used to stop the reaction at each time point. The 300 μL sample was centrifuged at 6000 rpm for 5 min; the supernatant was collected using a syringe and passed through a 0.45μm nylon membrane syringe filter. Control incubation containing all the constituents except the liver microsome was analyzed at 0, 30, 60, and 90-minute time points.

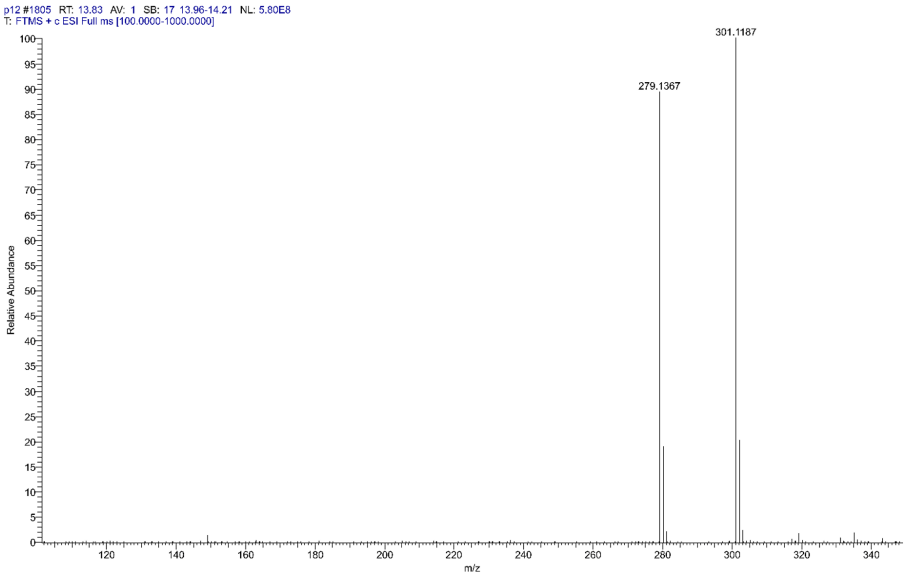

Figure 2 High resolution, positive mode HESI MS spectrum of (*E*)-2-[(4-methoxyphenyl) methylene]-1-benzosuberone (**2c**). (Protonated m/z 279.1367 and Na^+-adduct m/z 301.1187).

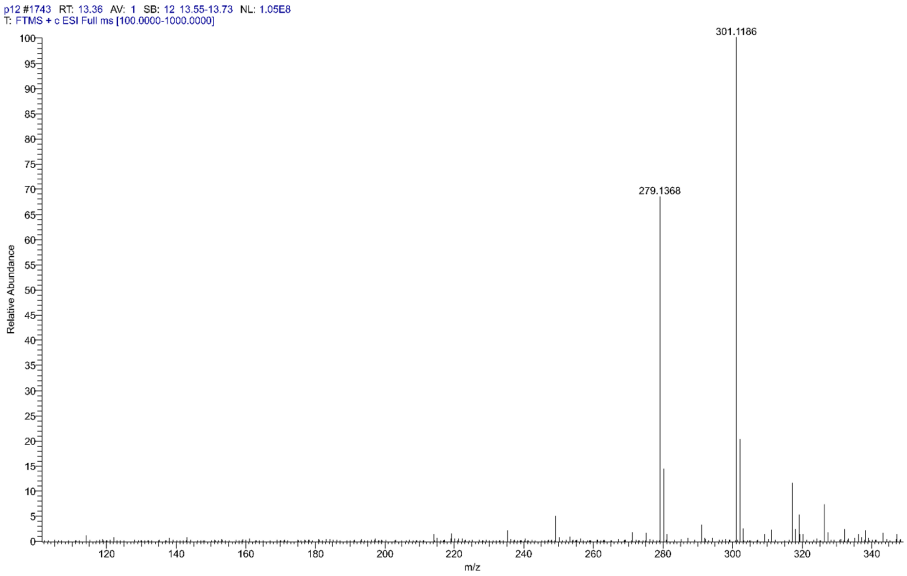

Figure 3 High resolution, positive mode HESI MS spectrum of (*Z*)-2-[(4-methoxyphenyl) methylene]-1-benzosuberone (**2c**). (Protonated m/z 279.1368 and Na^+-adduct m/z 301.1186).

2.4 HPLC-UV-MS measurements

HPLC-UV-ESI-MS analyses were performed on an Ultimate 3000 liquid chromatograph (Dionex, Sunnyvale, CA, USA) coupled with a Thermo Q Exactive Focus quadrupole-Orbitrap hybrid mass spectrometer (Thermo Fisher Scientific, Waltham, MA, USA). The scan monitored *m/z* values ranging from 100 to 1000 Da. Data acquisition was carried out using Q Exactive Focus 2.1 and Xcalibur 4.2 software (Thermo Fisher Scientific). Analysis of compounds and adducts was performed in HESI positive and negative ionization modes with the following parameters: spray voltage, 3500 V; vaporizer temperature, 300 °C; capillary temperature, 350 °C; spray and auxiliary gas flows, 30 and 10 arbitrary units, respectively; resolution, 35,000 at 200 *m/z*.

The parameters of the gradient were (A) water and 0.1% formic acid and (B) methanol and 0.1% formic acid. The gradient elution was as follows: isocratic elution for 1 min to 10% eluent B, continued by a linear gradient to 95% in 13 min, followed by an isocratic plateau for 3 min. Finally, the column was equilibrated to 10% in 0.1 min and continued isocratically for 2.9 min. The sampler was at room temperature, and the column oven was at 40 °C. The diode array detector was also set at 260, 280, 300, and 350 nm wavelength alongside MS analysis.

3 Results and discussion

Cytotoxic (antimitotic, cell growth inhibitor) effects of α,β-unsaturated carbonyl compounds are frequently associated with their expected reactivity with the essential thiol groups in living organisms [3–5, 26, 27]. Such a reaction can alter intracellular redox status (redox signaling), which can modulate events such as DNA synthesis, enzyme activation, selective gene expression, and cell cycle regulation [28, 29]. Several biological effects (e.g., NQO1 inducer [30], anti-inflammatory [31], GST P1-1 inhibitory [32]) of chalcones have been associated with their Michael-type reactivity towards reduced glutathione.

Microsomal incubation of **2c** was performed using alamethicin-activated rat liver microsomes. Alamethicin is a peptide antibiotic that forms voltage-dependent channels in the lipid bilayers by oligomerizing various alamethicin molecules [33]. The effect of alamethicin on the implementation rate for in vitro glucuronidation was previously studied by several authors [34–36]. It was found that alamethicin leads to an increase in metabolite formation. The authors assumed that the alamethicin forms a channel through the microsomal (endoplasmic reticulum) membranes, and the substrates may diffuse more easily into and through it. Accordingly, the formation of Phase 2 metabolites (such as glucuronides) is enhanced. Further studies showed that using alamethicin as an activator does not affect the microsomal CYP activities [37, 38].

In the first three minutes of the experiments, **2c** were incubated with rat liver microsomes in the presence of alamethicin. Since the parent compound does not have hydroxyl substituent, only the oxidation and reduction reactions were expected over this period. Then, GSH was added to the mixtures. From then on, reaction with GSH of the parent compound and its possible oxidative metabolites could also occur. These latter derivatives could be formed in spontaneous or GST-catalyzed reactions.

In earlier work, the non-enzyme-catalyzed reaction of **2c** with GSH was investigated by HPLC-UV. In that reaction, formation of four diastereomeric adducts was expected (Figure 4). Two of them result from a *cis*-, and another two from a *trans*-addition of GSH onto the carbon-carbon double bond. Under the used HPLC conditions, however, only two separated peaks appeared in the chromatograms. The separated peaks were tentatively assigned to the *cis*- and the *trans*-adducts [11].

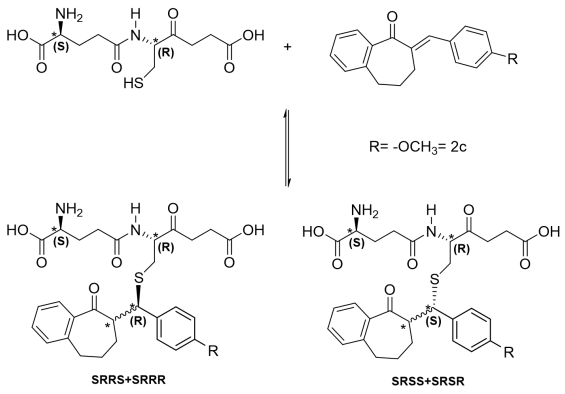

Figure 4 Structure and stereochemistry of the **2c-GSH** adducts

HPLC-MS investigation of the control incubates (without adding microsomes) indicated formation of the expected **2c-GSH** adducts (Table 1). Under the present chromatographic conditions, similar to the previous results, two separated chalcone-GSH peeks appeared in the chromatograms (Figure 5 lower panel). The structure of the **2c-GSH**-adducts (**2c-GSH-1** and **2c-GSH-2**) was verified by positive mode HR-MS (Figure 6 and 7).

Table 1 HPLC-MS peak areas (AUCs) of the **2c** and the **2c-GSH** isomeric peak as a function of incubation time

Sample	Area **2c-GSH**-1	Area **2c-GSH-2**	Area **2c-GSH-1** + **2c-GSH-2**	Area (***Z***)**-2c**	Area (***E***)**-2c**
Microsomal incubation (0 min)	2,210,842	4,293,434	6,504,276	856,426,548	8,297,984,438
Microsomal incubation (30 min)	22,983,588	32,617,903	55,601,491	966,438,207	4,610,557,010
Microsomal incubation (60 min)	22,454,721	29,934,874	52,389,595	524,872,308	2,750,174,832
Microsomal incubation (90 min)	50,714,479	61,666,740	112,381,219	550,348,953	3,815,982,269
Control (0 min)	1,466,946	2,493,046	3,959,992	495,826,994	4,093,677,464
Control (30 min)	1,396,532	1,181,043	2,577,575	138,997,108	1,308,801,409
Control (60 min)	9,585,848	5,960,060	15,545,908	161,346,308	1,305,287,139
Control (90 min)	18,724,489	12,017,553	30,742,042	299,494,818	2,215,039,743

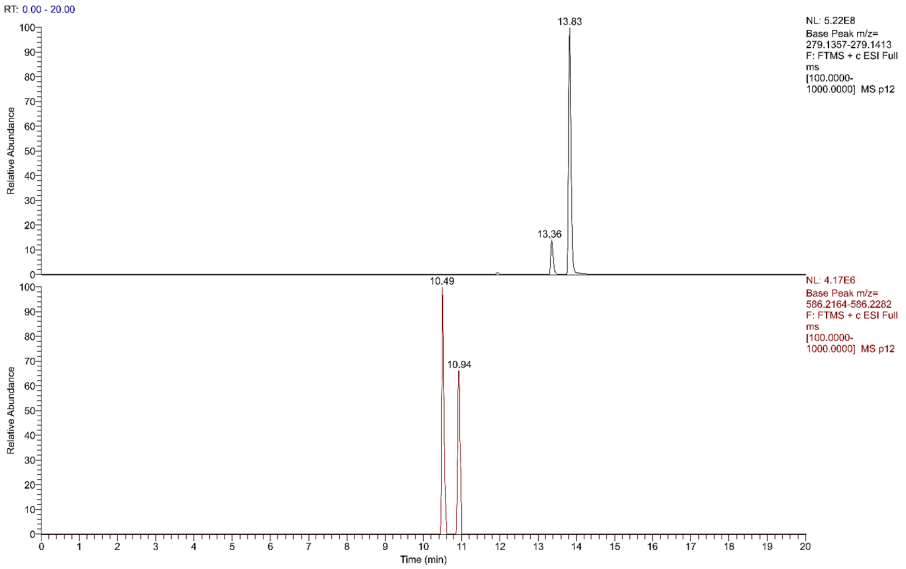

Figure 5 High resolution, positive mode HESI MS chromatogram of (*E*)-2-[(4-methoxyphenyl)methylene]-1-benzosuberone (**2c**) control incubate (90-minute sample). Upper panel: t_r 13.36 min: (*Z*)-2-[(4-methoxyphenyl)methylene]-1-benzo suberone; t_r 13.83 min: (*E*)-2-[(4-methoxyphenyl)methylene]-1-benzosuberone. Lower panel: **2c-GSH-1**: 10.49 min.; **2c-GSH-2**: 10.94 min.

Besides the GSH conjugates, formation of the respected (*Z*)-isomer of the parent **(*E*)-2c** was observed. Since the reaction mixtures were kept in the dark, the formation of the **(*Z*)-2c** can only be explained due to the retro-Michael reaction of the formed adducts [39]. The structure of the **(*E*)-2c** and **(*Z*)-2c** was verified based on the positive mode HR-MS of the isomeric mixture obtained by light isomerization f the pure **(*E*)-2c** (Figure 3).

Similar HPLC-MS analysis of the microsomal incubates also indicated formation of the **(*Z*)-2c** and the diastereomeric **2c-GSH** adducts (Figure 8). The mass spectra of the compounds formed in the microsomal incubations are shown in Figure 9-11. The sum of the AUC of the two diastereomeric **2c-GSH** peaks was higher at each timepoint than in the respective control incubate (Table 1). Although the ionization response factors of the four diastereomers are not known, the significant differences between the AUCs measured in the control and the microsomal incubates strongly support that the alamethicin-activated microsomes accelerate the chalcone-GSH conjugation reaction (Table 1). Since compound **2c** is a relatively lipophilic chalcone analog [40], it could be the substrate of both the microsomal glutathione transferases (MGSTs) [41–44] and the so-called microsome-associated GST enzymes. These latter GST forms are associated with the outer microsomal membranes, and their characteristics resemble those of the cytosolic GSTs [45].

Over the first 60 minutes of the incubation period, the total AUC of **2c-GSH** was only slightly changed (Table 1). However, by the end of the incubation, much higher AUC peak values of

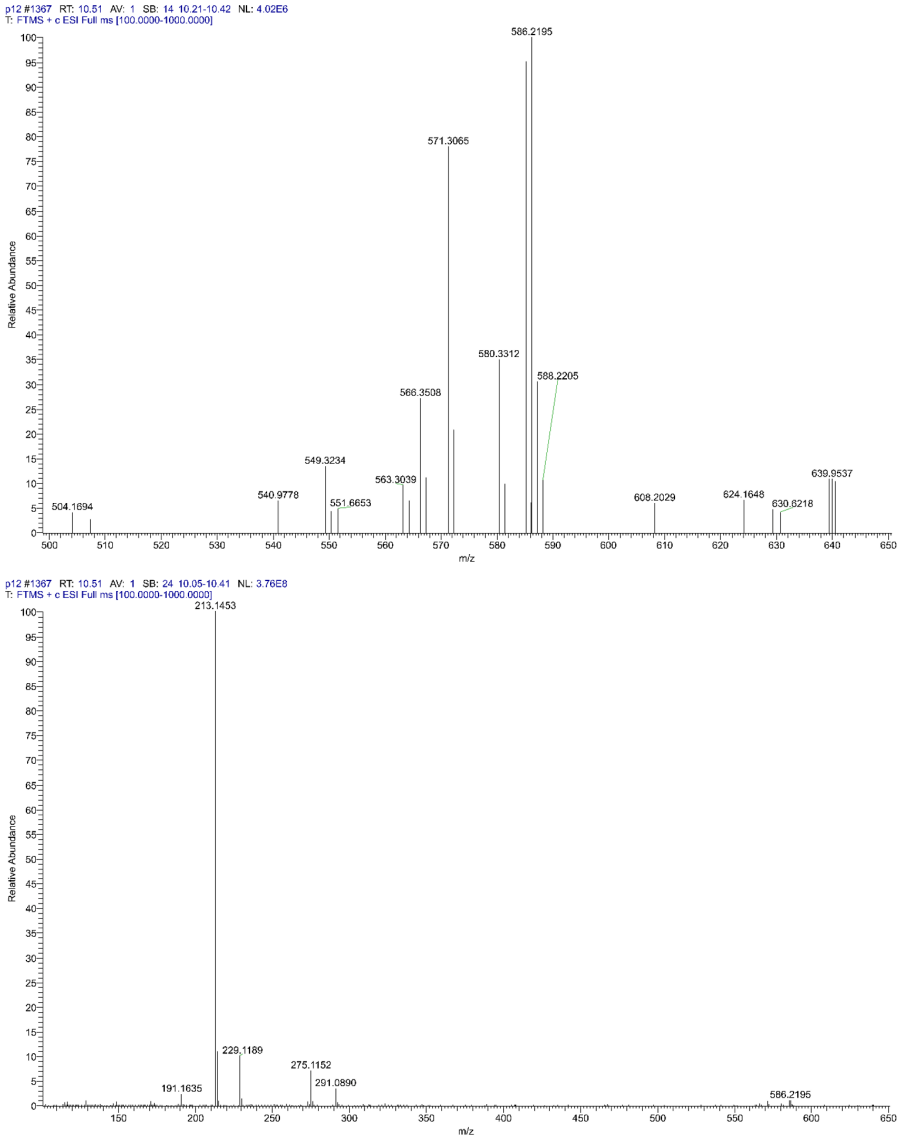

Figure 6 High resolution, positive mode HESI MS spectrum of the **2c-GSH-1** conjugate formed in the 90-minute sample of the control incubate (m/z 586.2195).

the **2c-GSH** conjugates could be observed (Table 2). On longer incubation times, dissolution of **2c** and GSH into the microsomal (ER) membranes can occur. There they can bind to the overlapping hydrophobic and the GSH binding sites of the MSGT enzymes [46]. In parallel, the added GSH can react with the enzyme's Cys49 sensor, resulting in its activation [47]. On activation of the MSGT enzymes, the reaction rate between the **2c** and GSH increased.

Liver microsomes are rich in cytochrome P450 enzymes. CYPs are located in the smooth endoplasmic reticulum membrane of cells. Thus, they can be recovered in microsomal fractions. Microsomal P450 families 1-3 play a major role in the metabolism of the majority of pharmaceuticals and a large number of other lipophilic xenobiotics [48]. CYP enzymes preferentially incorporate one of the oxygen atoms of molecular oxygen at one of the carbon atoms of the target molecule. Accordingly, chalcone **2c** possesses several possible primary sites for CYP-catalyzed oxidation.

In analysis of the total ion MS spectrum of the microsomal incubates, two products were found whose formation can be explained by CYP-catalyzed reactions: an oxygenated **2c (2c+O)** (Figure 12 and 13) and the demethylated derivative (**2c-CH$_2$**) (Figure 14 and 15). The AUC of both peaks increased over the incubation time (Table 2). The exact structure of the formed oxygenated metabolite needs further investigation. Lack of formation of a GSH-adduct of the possible epoxide metabolite, however, it is reasonable to suppose that the formed oxygenated metabolite is a hydroxyl derivative of **2c**. The demethylation reaction of **2c** resulted in the respective 4'-OH derivative (Figure 16).

Earlier studies on the 4'-OH-metabolite (**2c-CH$_2$**) showed the compound to have a pro-

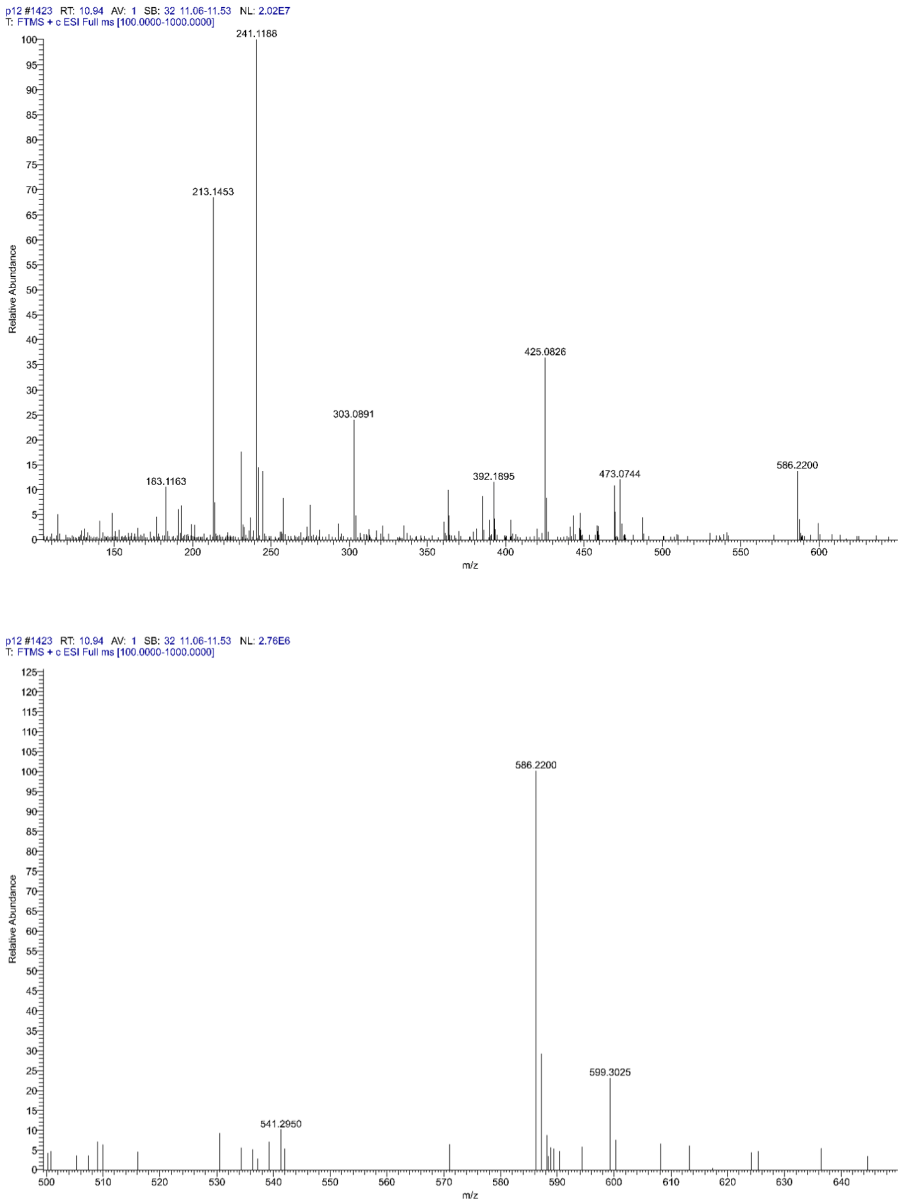

Figure 7 High resolution, positive mode HESI MS spectrum of the **2c-GSH-2** conjugate formed in the 90-minute sample of the control incubate (m/z 586.2200).

nounced effect on the modulation of mitochondrial respiratory functions. Phosphorylation inhibitory effect and/or partial uncoupling of the compound resulted in stimulation of mitochondrial activity and increased formation of ROS [49].

Okamoto *et al.* reported the reduction of (*E*)-4-phenyl-3-buten-2-one (a chalcone analog) by rat microsomal carbonyl reductase. The reduction was stereoselective, yielding *R*-(*E*)-4-phenyl-3-buten-2-ol [14]. Based on this finding, the total ion MS spectrum of the 90-minute microsomal incubate was screened for the presence of the respective reduced form of **2c**. The analysis didn't indicate the presence of a signal of the corresponding alcohol.

4 Conclusions

Microsomal biotransformation of the antiproliferative (*E*)-2-[(4'-methoxyphenyl)methylene]-benzosuberon-1-one (**2c**) showed the compound to be metabolized by the CYP and the GST enzymes. As a result of CYP-catalyzed transformations, one monooxygenated (**2c+O**) and the demethylated (**2c-CH$_2$**) metabolites were identified. Microsomal GST-catalyzed reaction of the compound resulted in formation of diastereomeric GST-conjugates. Under the present HPLC conditions, the compounds were separated into two chromatographic peaks. A noticeable amount of **(*Z*)-2c** was also identified in the incubates. Since the (*Z*)-isomer of the parent compound has a different three-dimensional structure, degree of conjugation, and lipophilicity [50],

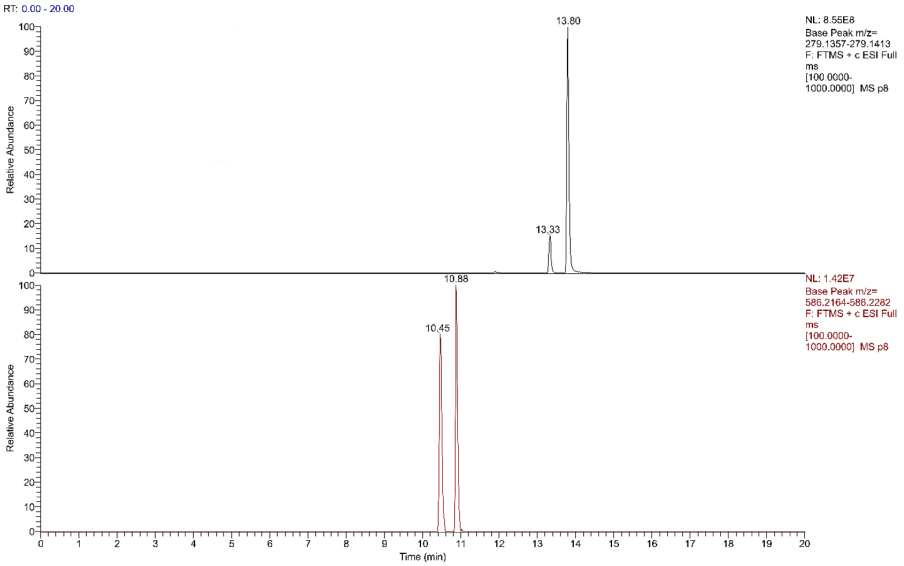

Figure 8 High resolution, positive mode HESI MS chromatogram of (*E*)-2-[(4-methoxyphenyl)methylene]-1-benzosuberone (**2c**) microsomal incubate (90-minute sample). Upper panel: t_r 13.33 min: (*Z*)-2-[(4-methoxyphenyl) methylene]-1-benzosuberone; t_r 13.80 min: (*E*)-2-[(4-methoxyphenyl)methylene]-1-benzosuberone. Lower panel: **2c-GSH-1**: 10.45 min.; **2c-GSH-2**: 10.88 min.

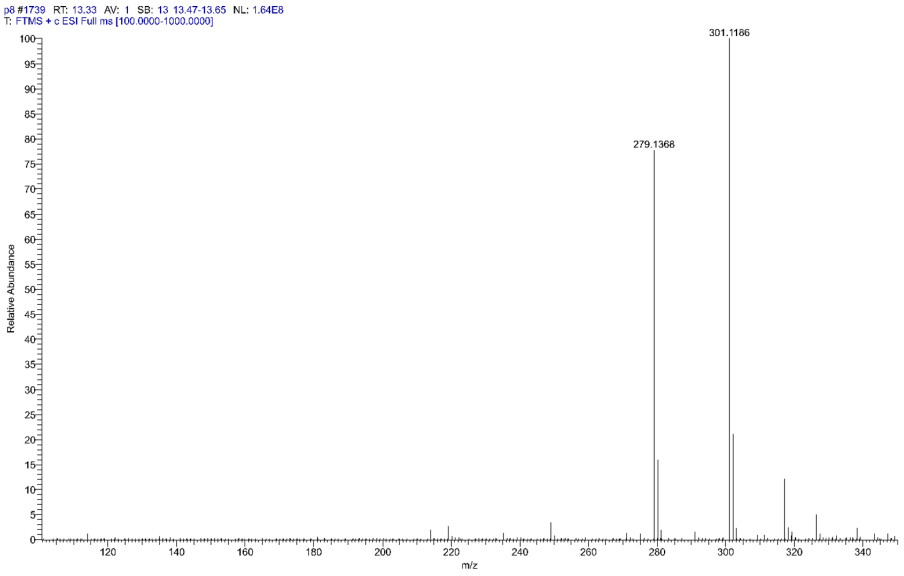

Figure 9 High resolution, positive mode HESI MS spectrum of (*Z*)-2-[(4-methoxyphenyl) methylene]-1-benzosuberone (**2c**) formed in the 90-minute sample of the microsomal incubate. (Protonated m/z 279.1368 and Na^+-adduct m/z 301.1186).

Table 2 HPLC-MS peak areas (AUCs) of the **2c**, the **2c-GSH** isomeric peaks, and that of the oxidative metabolites of **2c** as a function of incubation time.

Compound	t_r (min)	Control (0 min)	Control (90 min)	Microsome (0 min)	Microsome (90 min)
(*E*)-2c	13.8	4,093,677,464	2,215,039,743	8,297,984,438	3,815,982,269
(*Z*)-2c	13.32	495,826,994	299,494,818	856,426,548	550,348,953
2c-GSH-1	10.47	1,466,946	18,724,489	2,210,842	50,714,479
2c-GSH-2	10.86	2,493,046	12,017,553	4,293,434	61,264,226
2c-CH_2	12.25	N/D	N/D	7,206,428	81,441,916
2c+O	11.93	N/D	N/D	11,740,789	44,057,081

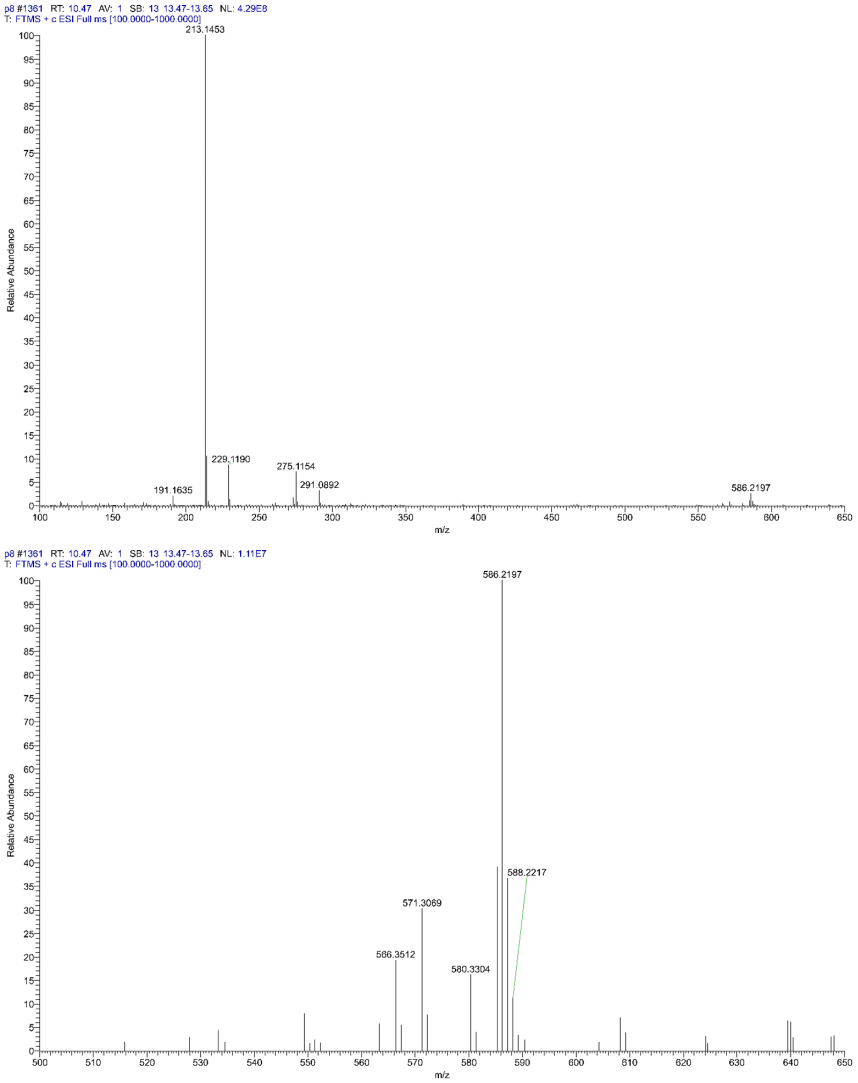

Figure 10 High resolution, positive mode HESI MS spectrum of the **2c-GSH-1** conjugate formed in the 90-minute sample of the microsomal incubate (m/z 586.2197).

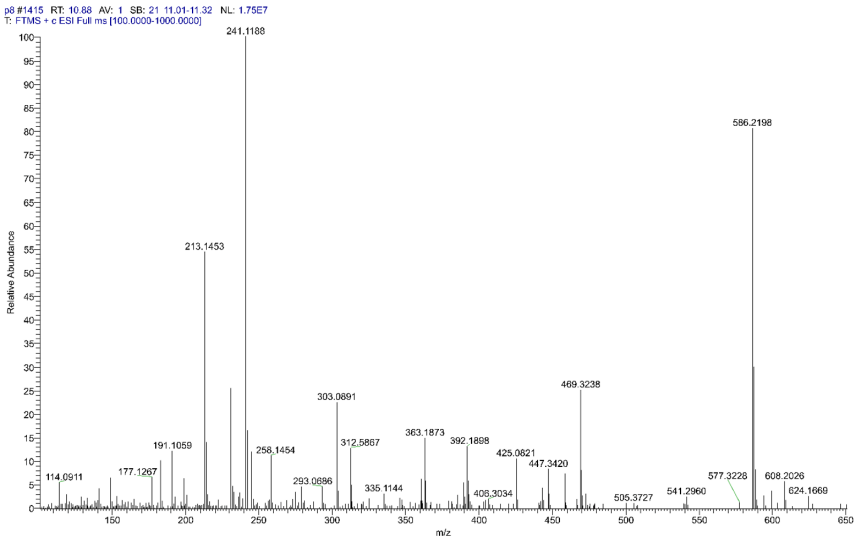

Figure 11 High resolution, positive mode HESI MS spectrum of the **2c-GSH-2** conjugate formed in the 90-minute sample of the microsomal incubate (m/z 586.2198).

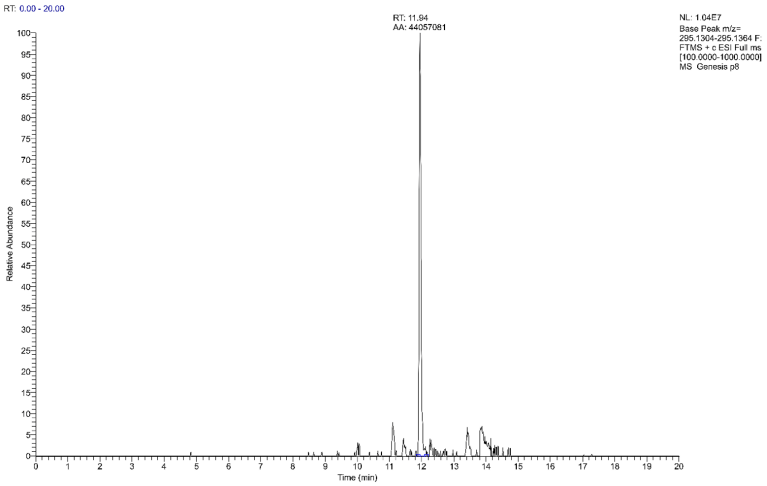

Figure 12 High resolution, positive mode HESI MS chromatogram of the monohydroxylated derivative of (*E*)-2-[(4-methoxyphenyl)methylene]-1-benzosuberone (**2c**) formed in the 90-minute sample of the microsomal incubate. (t_r 11.94 min).

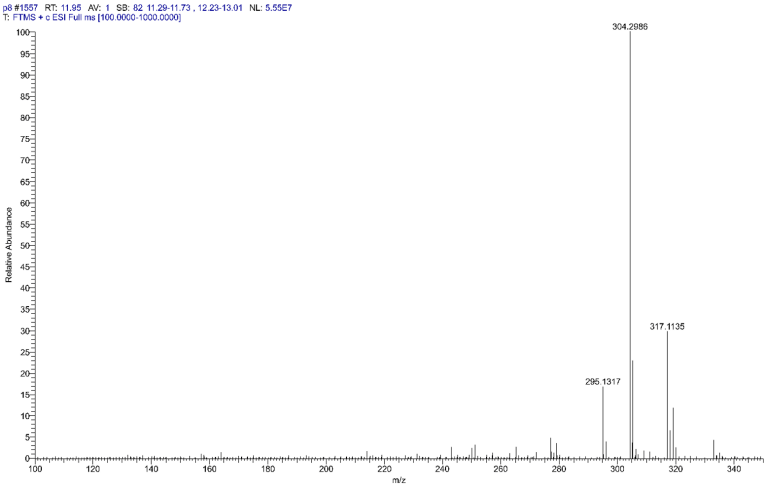

Figure 13 High resolution, positive mode HESI MS spectrum of the monohydroxylated derivative of (*E*)-2-[(4-methoxyphenyl)methylene]-1-benzosuberone (**2c**) formed in the 90-minute sample of the microsomal incubate. (Protonated m/z 295.1317 and Na^+-adduct m/z 317.1135)

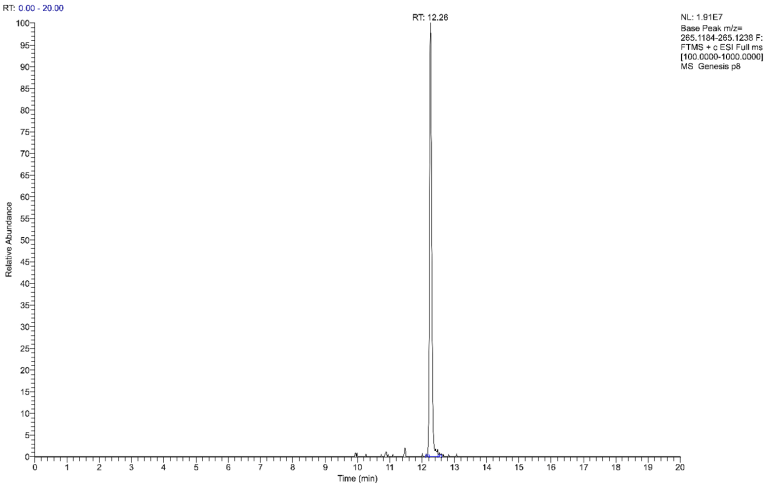

Figure 14 High resolution, positive mode HESI MS chromatogram of the O-demethylated derivative of (*E*)-2-[(4-methoxyphenyl)methylene]-1-benzosuberone (**2c**) formed in the 90-minute sample of the microsomal incubate. (t_r 12.26 min).

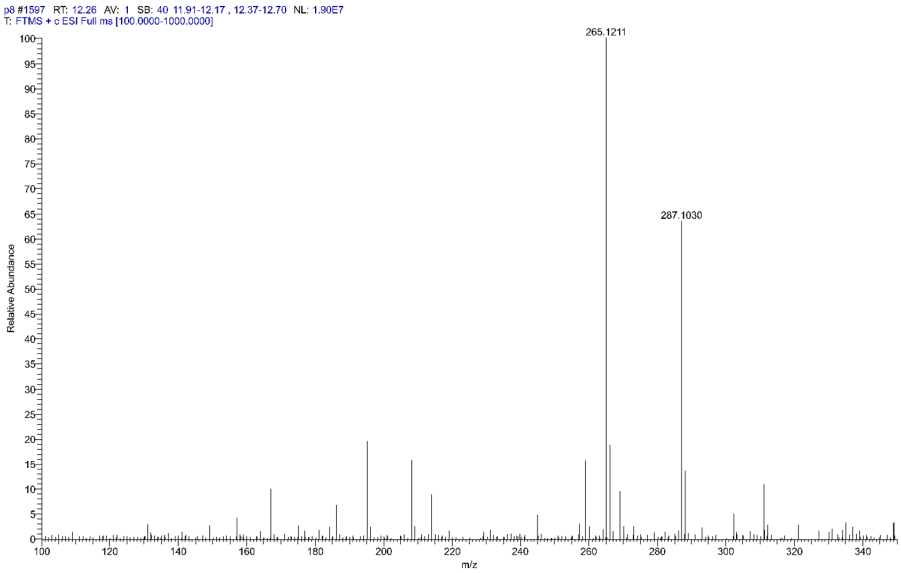

Figure 15 High resolution, positive mode HESI MS spectrum of of the O-demethylated derivative of (*E*)-2-[(4-methoxyphenyl)methylene]-1-benzosuberone (**2c**) formed in the 90-minute sample of the microsomal incubate. (Protonated m/z 265.1213 and Na^+-adduct m/z 287.1030).

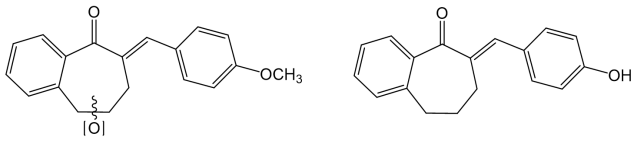

Figure 16 Structures of the products formed in the microsomal oxidation of **2c**

formation of this isomer might be a molecular event that plays a role in the observed biological effects of the compound. Furthermore, the GSH-reactivity of **2c** can also take part in the previously reported apoptotic effect of the compound.

References

[1] Part XVI, Rozmer Z and Perjesi P. (*E*)-2-Benzylidenecyclanones: Part XVI. Study on the interaction of some (*E*)-2-benzyldenebenzosuberone derivatives with serum albumin by UV-Vis method, inhibitory effect on topoisomerase. Journal of Pharmaceutical and Biopharmaceutical Research, 2020, **2**(1):118-125. https://doi.org/10.25082/JPBR.2020.01.003

[2] Rozmer Z and Perjési P. Naturally occurring chalcones and their biological activities. Phytochemistry Reviews, 2016, **15**(1): 87-120. https://doi.org/10.1007/s11101-014-9387-8

[3] Mahapatra DK, Bharti SK and Asati V. Anti-cancer chalcones: Structural and molecular target perspectives. European Journal of Medicinal Chemistry, 2015, **98**: 69-114. https://doi.org/10.1016/j.ejmech.2015.05.004

[4] Zhuang C, Zhang W, Sheng C, *et al*. Chalcone: a privileged structure in medicinal chemistry. Chemical reviews, 2017, **117**(12): 7762-7810. https://doi.org/10.1021/acs.chemrev.7b00020

[5] Gomes MN, Muratov EN, Pereira M, *et al*. Chalcone Derivatives: Promising starting points for drug design. Molecules, 2017, **22**(8): 1210. https://doi.org/10.3390/molecules22081210

[6] Dimmock JR, Kandepu NM, Nazarali AJ, *et al*. Conformational and quantitative structure-activity relationship study of cytotoxic 2-arylidenebenzocycloalkanones. Journal of Medicinal Chemistry, 1999, **42**(8): 1358-1366. https://doi.org/10.1021/jm9806695

[7] Dimmock JR, Zello GA, Oloo EO, *et al*. Correlations between cytotoxicity and topography of some 2-arylidenebenzocycloalkanones determined by X-ray crystallography. Journal of Medicinal Chemistry, 2002, **45**(14): 3103-3111. https://doi.org/10.1021/jm010559p

[8] Perjési P, Das U, De Clercq E, *et al*. Design, synthesis and antiproliferative activity of some 3-benzylidene-2,3-dihydro-1-benzopyran-4-ones which display selective toxicity for malignant cells. European Journal of Medicinal Chemistry, 2007, **43**(4): 839-845. https://doi.org/10.1016/j.ejmech.2007.06.017

[9] Rozmer Z, Berki T and Perjési P. Different effects of two cyclic chalcone analogues on cell cycle of Jurkat T cells. Toxicology in Vitro, 2006, **20**(8): 1354-1362. https://doi.org/10.1016/j.tiv.2006.05.006

[10] Pilatova M, Varinska L, Perjesi P, *et al*. In vitro antiproliferative and antiangiogenic effects of synthetic chalcone analogues. Toxicology in Vitro, 2010, **24**(5): 1347-1355. https://doi.org/10.1016/j.tiv.2010.04.013

[11] Perjési P, Maász G, Reisch R, *et al*. (*E*)-2-Benzylidenebenzocyclanones: Part VII. Investigation of the conjugation reaction of two cytotoxic cyclic chalcone analogues with glutathione: an HPLC–MS study. Monatshefte für Chemie, 2012, **143**(8): 1107-1114. https://doi.org/10.1007/s00706-012-0768-7

[12] Rozmer Z, Berki T, Maász G, *et al*. Different effects of two cyclic chalcone analogues on redox status of Jurkat T cells. Toxicology in Vitro, 2014, **28**(8):1359-1365. https://doi.org/10.1016/j.tiv.2014.06.006

[13] Kohno Y, Kitamura S, Sanoh S, *et al*. Metabolism of the α,β-unsaturated ketones, chalcone and trans -4-phenyl-3-buten-2-one, by rat liver microsomes and estrogenic activity of the metabolites. Drug Metabolism and Disposition, 2005, **33**(8): 1115-1123. https://doi.org/10.1124/dmd.104.002634

[14] Okamoto Y, Kitamura S, Takeshita M, *et al*. Microsomal carbonyl reductase responsible for reduction of 4-phenyl-3-buten-2-one in rats. IUBMB Life, 1999, 48(5): 543-547. https://doi.org/10.1080/713803550

[15] Huang L, Nikolic D and van Breemen RB. Hepatic metabolism of licochalcone A, a potential chemopreventive chalcone from licorice (Glycyrrhiza inflata), determined using liquid chromatography-tandem mass spectrometry. Analytical and Bioanalytical Chemistry, 2017, **409**(30): 6937-6948. https://doi.org/10.1007/s00216-017-0642-x

[16] Nikolic D, Li Y, Chadwick LR, *et al*. Metabolism of 8-prenylnaringenin, a potent phytoestrogen from hops (Humulus lupulus), by human liver microsomes. Drug metabolism and disposition, 2004, **32**(2): 272-279. https://doi.org/10.1124/dmd.32.2.272

[17] Bernardes A, Kuzma M, Almási A, *et al*. HPLC and HPLC-MS analysis of intestinal elimination and phase 2 metabolism of 4'-hydroxy-4-methoxychalcone and its bis-Mannich analog in the rat. The Open Medicinal Chemistry Journal, 2022, **16**(1): e187410452208110. https://doi.org/10.2174/18741045-v16-e2208110

[18] Bernardes A, Pérez CN, Mayer M, *et al*. Study of reactions of two Mannich bases derived of 4'-hydroxychalcones with glutathione by RP-TLC, RP-HPLC and RP-HPLC-ESI-MS analysis. Journal of the Brazilian Chemical Society, 2017, **28**: 1048-1062. https://doi.org/10.21577/0103-5053.20160260

[19] Jones DP. Redox potential of GSH/GSSG couple: Assay and biological significance. In: Methods in Enzymology (Internet). Elsevier, 2002, 93-112. https://doi.org/10.1016/s0076-6879(02)48630-2

[20] Aw TY. Cellular Redox: A Modulator of Intestinal Epithelial Cell Proliferation. Physiology, 2003, **18**(5): 201-204. https://doi.org/10.1152/nips.01448.2003

[21] Schafer FQ and Buettner GR. Redox environment of the cell as viewed through the redox state of the glutathione disulfide/glutathione couple. Free Radical Biology and Medicine, 2001, **30**(11): 1191-1212. https://doi.org/10.1016/s0891-5849(01)00480-4

[22] Perjési P. Glutathione: biosynthesis, functions and biological implications. Nova Science Publishers, New York, 2019. ISBN 978-1-53614-740-7.

[23] Hill JR. In vitro drug metabolism using liver microsomes. Current Protocols in Pharmacology, 2004. https://doi.org/10.1002/0471141755.ph0708s23

[24] Perjési P, Nusser T, Tarczay Gy, *et al*. *E*-2-Benzylidenebenzocycloalkanones. Stereostructure and NMR spectroscopic investigation. Journal of Molecular Structure, 1999, **479**(1): 13-19. https://doi.org/10.1016/S0022-2860(98)00805-9

[25] Phosphate-Buffered Saline (PBS; 0.1 M, pH 7.4). Cold Spring Harbor Protocols, 2014, **2014**(12): pdb.rec085126. https://doi.org/10.1101/pdb.rec085126

[26] Karthikeyan C, Narayana Moorthy NSH, Ramasamy S, *et al*. Advances in Chalcones with Anticancer Activities. Physical Review A, 2014, **10**(1): 97-115. https://doi.org/10.2174/1574892809666140819153902

[27] Constantinescu T and Mihis AG. Two Important Anticancer Mechanisms of Natural and Synthetic Chalcones. International Journal of Molecular Sciences, 2022, **23**(19): 11595. https://doi.org/10.3390/ijms231911595

[28] Powis G, Gasdaska JR and Baker A. Redox signaling and the control of cell growth and death. Advances in pharmacology, 1996, **38**: 329-359. https://doi.org/10.1016/s1054-3589(08)60990-4

[29] Vašková J, Kočan L, Vaško L, *et al*. Glutathione-Related Enzymes and Proteins: A Review. Molecules, 2023, **28**(3): 1447.
https://doi.org/10.3390/molecules28031447

[30] Dinkova-Kostova AT, Massiah MA, Bozak RE, *et al*. Potency of Michael reaction acceptors as inducers of enzymes that protect against carcinogenesis depends on their reactivity with sulfhydryl groups. Proceedings of the National Academy of Sciences, 2001, **98**(6):3 404-309.
https://doi.org/10.1073/pnas.051632198

[31] Jin YL, Jin XY, Jin F, *et al*. Structure activity relationship studies of anti-inflammatory TMMC derivatives: 4-Dimethylamino group on the B ring responsible for lowering the potency. Archives of Pharmacal Research 2009, **31**(9): 1145.
https://doi.org/10.1007/s12272-001-1281-7

[32] Wang J, Wang S, Song D, *et al*. Chalcone Derivatives Inhibit Glutathione S-Transferase P1-1 Activity: Insights into the Interaction Mode of α,β-Unsaturated Carbonyl Compounds. Chemical biology & drug design, 2009, **73**(5): 511-514.
https://doi.org/10.1111/j.1747-0285.2009.00807.x

[33] Leitgeb B, Szekeres A, Manczinger L, *et al*. The history of alamethicin: a review of the most extensively studied peptaibol. Chemistry & biodiversity, 2007, **4**(6): 1027-1051.
https://doi.org/10.1002/cbdv.200790095

[34] Fisher MB, Campanale K, Ackermann BL, *et al*. In vitro glucuronidation using human liver microsomes and the pore-forming peptide alamethicin. Drug metabolism and disposition, 2000, **28**(5): 560-566.

[35] Kumar S, Samuel K, Subramanian R, *et al*. Extrapolation of diclofenac clearance from in vitro microsomal metabolism data: role of acyl glucuronidation and sequential oxidative metabolism of the acyl glucuronide. Journal of Pharmacology and Experimental Therapeutics, 2002, **303**(3): 969-978.
https://doi.org/10.1124/jpet.102.038992

[36] Walsky RL, Bauman JN, Bourcier K, *et al*. Optimized assays for human UDP-glucuronosyltransferase (UGT) activities: altered alamethicin concentration and utility to screen for UGT inhibitors. Drug Metabolism and Disposition, 2012, **40**(5): 1051-1065.
https://doi.org/10.1124/dmd.111.043117

[37] Boase S and Miners JO. In vitro–in vivo correlations for drugs eliminated by glucuronidation: investigations with the model substrate zidovudine. British Journal of Clinical Pharmacology, 2002, **54**(5): 493-503.
https://doi.org/10.1046/j.1365-2125.2002.01669.x

[38] Yan Z and Caldwell GW. Metabolic assessment in liver microsomes by co-activating cytochrome P450s and UDP-glycosyltransferases. European Journal of Drug Metabolism and Pharmacokinetics, 2003, **28**(3): 223-232.
https://doi.org/10.1007/BF03190489

[39] Berne D, Ladmiral V, Leclerc E, *et al*. Thia-Michael reaction: The route to promising covalent adaptable networks. Polymers, 2022, **14**(20): 4457.
https://doi.org/10.3390/polym14204457

[40] Rozmer Z, Perjési P and Takács-Novák K. Application of RP-TLC for logP determination of isomeric chalcones and cyclic chalcone analogues. Journal of Planar Chromatography — Modern TLC, 2006, **19**: 124-128.
https://doi.org/10.1556/jpc.19.2006.2.7

[41] Lundqvist G, Yücel-Lindberg T and Morgenstern R. The oligomeric structure of rat liver microsomal glutathione transferase studied by chemical cross-linking. Biochimica et Biophysica Acta (BBA)-Protein Structure and Molecular Enzymology, 1992, **1159**(1): 103-108.
https://doi.org/10.1016/0167-4838(92)90081-n

[42] Jakobsson PJ, Mancini JA, Riendeau D, *et al*. Identification and characterization of a novel microsomal enzyme with glutathione-dependent transferase and peroxidase activities. Journal of Biological Chemistry, 1997, **272**(36): 22934-22939.
https://doi.org/10.1074/jbc.272.36.22934

[43] Jakobsson PJ, Morgenstern R, Mancini J, *et al*. Common structural features of MAPEG—a widespread superfamily of membrane associated proteins with highly divergent functions in eicosanoid and glutathione metabolism. Protein Science, 1999, **8**(3): 689-692.
https://doi.org/10.1110/ps.8.3.689

[44] Weinander R, Ekström L, Andersson C, *et al*. Structural and Functional Aspects of Rat Microsomal Glutathione Transferase. Journal of Biological Chemistry, 1997, **272**(14): 8871-8877.
https://doi.org/10.1074/jbc.272.14.8871

[45] Morgenstern R, Guthenberg C, Mannervik B, *et al*. The amount and nature of glutathione transferases in rat liver microsomes determined by immunochemical methods. FEBS letters, 1983, **160**(1-2): 264-268.
https://doi.org/10.1016/0014-5793(83)80979-x

[46] Busenlehner LS, Ålander J, Jegerscöhld C, *et al*. Location of substrate binding sites within the integral membrane protein microsomal glutathione transferase-1. Biochemistry 2007, **46**(10): 2812-2822.
https://doi.org/10.1021/bi6023385

[47] Morgenstern R, Depierre JW and Ernster L. Activation of microsomal glutathione S-transferase activity by sulfhydryl reagents. Biochemical and Biophysical Research Communications, 1979, **87**(3): 657-663.
https://doi.org/10.1016/0006-291x(79)92009-6

[48] Parkinson A, Ogilvie BW, Buckley DB, *et al*. Biotransformation of Xenobiotics. In "Casarett and Doull's Toxicology: The Basic Science of Poisons (Editor: C. D. Klassen). 9th edition. McGraw Hill, 2019.

[49] Guzy J, Vasková-Kubalkova J, Rozmer Z, *et al*. Activation of oxidative stress response by hydroxyl substituted chalcones and cyclic chalcone analogues in mitochondria. FEBS Letters, 2010, **584**: 567-570.
https://doi.org/10.1016/j.febslet.2009.11.098

[50] Perjési P. (E)-2-benzylidenebenzocyclanones: Part XIII. Light-induced in solution (E)/(Z) isomerization of some cyclic chalcone analogues. Effect of ring size on lipophilicity of geometric isomers. Monatshefte der Chemie, 2015, **146**(8): 1275-1281.
https://doi.org/10.1007/s00706-015-1463-2